Inorg. Chem. **2007**, *46*, 7410–7413

Why Does the Disorder of *R*-pn and *rac*-pn Ligands in the Quasi-One-Dimensional Bromo-Bridged Ni^{III} Complexes, $[Ni(pn)_2Br]Br_2$ (pn = 1,2-diaminopropane) Afford Similar STM Patterns?

Hashen Wu,[†] Daisuke Kawakami,[†] Mari Sasaki,[†] Jimin Xie,[†] Shinya Takaishi,[†] Takashi Kajiwara,[†] Hitoshi Miyasaka,[†] Masahiro Yamashita,*[,†] Hiroyuki Matsuzaki,[‡] and Hiroshi Okamoto[‡]

Department of Chemistry, Faculty of Science, Tohoku University and CREST(JST), Aramaki-Aza-Aoba, Aoba-ku, Sendai 980-8578, Japan, and Department of Advanced Materials Science, Graduate School of Frontier Sciences, The University of Tokyo, Kashiwa 277-8561, Japan

Received February 28, 2007

The disordered patterns of *R*- and *rac*-1,2-diaminopropane (pn) in quasi-one-dimensional bromo-bridged Ni(III) complexes, $[Ni^{III}(pn)_2Br]Br_2$, have been investigated by single-crystal X-ray structure determination and scanning tunneling microscopy (STM). X-ray structure determination shows that the methyl moieties are disordered on the right- and left-hand sides with half occupancies in both compounds, while the carbon atoms of the ethylene moieties of pn ligands are disordered in $[Ni(rac\text{-}pn)_2Br]Br_2$ and not disordered in $[Ni(R\text{-}pn)_2Br]Br_2$. In the STM images of both compounds, the bright spots are not straight but fluctuated with the similar patterns. We have concluded that tunnel current from the STM tip to metal ions are detected via methyl groups of pn ligands.

Introduction

Quasi-one-dimensional compounds have attracted considerable attention due to their novel physical properties such as the Peierls transition, spin−Peierls transition, neutral−ionic transition, charge density wave (CDW) states, spin density wave (SDW) states, Mott−Hubbard (MH) states, superconductivities, etc.[1] Among these compounds, the quasi-one-dimensional halogen-bridged mixed-valence compounds (hereafter abbreviated as MX-chains) have been extensively investigated during the past 20 years, since they exhibit a wide range of interesting physical properties. These include intense and dichroic intervalence charge transfer (CT) bands,[2] progressive overtones of resonance Raman spectra,[3] luminescence spectra with large Stokes shifts,[4] mid-gap absorptions attributable to solitons and polarons,[5] large third-order nonlinear optical properties, one-dimensional model compounds of high-T_c copper-oxide superconductors, etc.[6] The third-order nonlinear optical susceptibilities ($\chi^{(3)}$) of these compounds are observed to be larger than that of poly(diacetylene) or poly(silane).[7] Indeed, recently a gigantic third-order optical nonlinear susceptibility has been observed in $[Ni(chxn)_2Br]Br_2$ ($\chi^{(3)} \approx 10^{-4}$ esu) (chxn = 1*R*,2*R*-diaminocyclohexane).[8]

From a theoretical viewpoint, the MX-chain compounds are regarded as Peierls−Hubbard systems. In such a system, the electron−phonon interaction (*S*), the electron-transfer energy (*T*), the on-site and intersite Coulomb interactions (*U* and *V*, respectively) compete and/or cooperate with one another.[9] Originally, these MX-chain compounds were regarded as a one-dimensional metallic state with half-filled

* To whom correspondence should be addressed. E-mail: yamasita@agnus.chem.tohoku.ac.jp.
† Tohoku University and CREST(JST).
‡ The University of Tokyo.

(1) *Extended Linear Chain Compounds*; Miller, J. S., Ed.; Plenum Press: New York, 1982; Vols. I−III.
(2) (a) Tanaka, M.; Kurita, S.; Kojima, T.; Yamada, Y. *Chem. Phys.* **1984**, *91*, 257−265. (b) Wada, Y.; Mitani, T.; Yamashita, M.; Koda, T. *J. phys. Soc. Jpn.* **1985**, *54*, 3143−3153.
(3) (a) Clark, R. J. H.; Franks, M. L.; Trumble, W. R. *Chem. Phys. Lett.* **1976**, *41*, 287−292. (b) Clark, R. J. H.; Kurmoo, M.; Mountney, D. N.; Toftlund, H. *J. Chem. Soc., Dalton Trans*. **1982**, 1851−1860 (c) Clark, R. J. H. *Adv. Infrared Raman Spectrosc.* **1983**, *11*, 95−130.
(4) Tanino, H.; Kobayashi, K. *J. Phys. Soc. Jpn.* **1983**, *52*, 1446−1456.
(5) (a) Okamoto, H.; Mitani, T.; Toriumi, K.; Yamashita, M. *Phys. Rev. Lett.* **1992**, *69*, 2248−2251. (b) Okamoto, H.; Yamashita, M. *Bull. Chem. Soc. Jpn.* **1998**, *71*, 2023−2039.
(6) Yamashita, M.; Yokoyama, K.; Furukawa, S.; Manabe, T.; Ono, T.; Nakata, K.; Kachi-Terajima, C.; Iwahori, F.; Ishii, T.; Miyasaka, H.; Sugiura, k.; Matsuzaki, H.; Kishida, H.; Okamoto, H.; Tanaka, H.; Hasegawa, Y.; Marumoto, K.; Ito, H.; Kuroda, S. *Inorg. Chem.* **2002**, *41*, 1998−2000.
(7) Iwasa, Y.; Funatsu, E.; Hasegawa, T.; Koda, T.; Yamashita, M. *Appl. Phys. Lett.* **1991**, *59*, 2219−2221.
(8) Kishida, H.; Matsuzaki, H.; Okamoro, H.; Manabe, T.; Yamashita, M.; Taguchi, Y.; Tokura, Y. *Nature*. **2000**, *405*, 929−932.

10.1021/ic700379m CCC: $37.00
Published on Web 07/31/2007

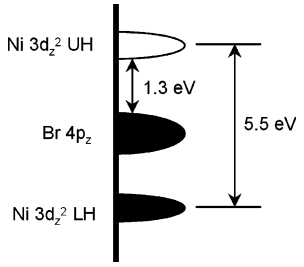

Figure 1. Schematic band structure of $[Ni(chxn)_2Br]Br_2$.

d_{z^2} orbitals of the metals and filled p_z orbitals of the bridging halides. However, it is well known that the one-dimensional metallic state is unstable and that the system is subsequently transferred to the insulating state via the *S* or the *U*. In most MX-chain compounds, due to the *S*, the bridging halides are displaced from the midpoints between the neighboring two metal atoms, giving rise to CDW states or $M^{II}-M^{IV}$ mixed-valence states ($\cdots M^{II}\cdots X-M^{IV}-X\cdots M^{II}\cdots$). Accordingly, the half-filled metallic band is split into an occupied valence band and an unoccupied conduction band with a finite Peierls gap. Therefore, these compounds belong to the class II type of the Robin−Day classification for the mixed-valence complexes.[10]

Theoretically, it has been proposed that the M^{III} state or MH state, in which the bridging halides are located at the midpoints between two neighboring metal ions ($-X-M^{III}-X-M^{III}-X-$), is stabilized when *U* is larger than *S*. Therefore, these compounds belong to the class III type of the Robin−Day classification.[10] We have succeeded in synthesizing a series of such compounds, formulated as $[Ni^{III}(chxn)_2X]Y_2$ (X = Cl, Br, or mixed halides; Y = Cl, Br, mixed halides, ClO_4, BF_4, or NO_3) for the first time. The choice of Ni is because the Ni ion has larger *U* compared with that of a Pd or Pt ion.[11] These Ni^{III} compounds showed a very strong antiferromagnetic interaction among spins located on $3d_{z^2}$ orbitals of each Ni^{III} ion throughout the bridging halides ($J \approx 2800$ K). Okamoto et al. have revealed the band structure of halogen-bridged Ni compounds by using the X-ray photoelectron spectrum (XPS), Auger electron spectrum (AES), and optical conductivity spectrum.[12] From XPS and AES, the *U* value was estimated to be ca. 5.5 eV ($U = E_{2p}(XPS) - 2E_{valence}(XPS) - E_k(AES)$), which is much larger than that of Pd (∼1.5 eV)[13] or Pt (∼1.0 eV)[14] systems. On the other hand, optical conductivity spectra showed an intense CT band at 1.3 eV, which is attributable to CT from bridging halide ions to upper Hubbard band of Ni. Therefore, the band structure can be schematically illustrated as in Figure 1. Since the energy levels of the bridging halides are located between the upper- and lower-Hubbard bands composed of the $Ni^{3+}d_{z^2}$ orbitals, these Ni compounds are strictly not in the Mott insulators, but in the CT insulators. Such a band structure is quite analogous to that of starting materials of the copper oxide superconductors (La_2CuO_4), except for the dimensionality of the electronic system.

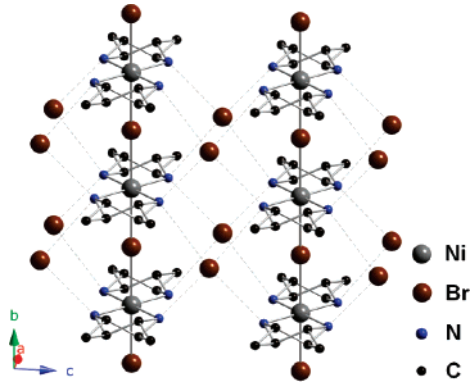

Figure 2. Crystal structure of $[Ni(rac\text{-}pn)_2Br]Br_2$. Hydrogen atoms are omitted for clarity. Dashed lines show hydrogen bonds between amino-protons and bromide ions.

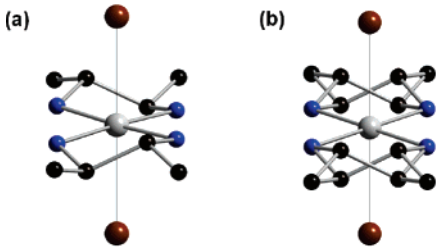

Figure 3. Disordered states of (a) $[Ni(R\text{-}pn)_2Br]Br_2$ and (b) $[Ni(rac\text{-}pn)_2Br]Br_2$.

Although many attempts on substituting bridging halide ions and counter-anions have so far been carried out in the Ni^{III} complexes, the substituting effect of the in-plane ligands has been limited. For the application of $\chi^{(3)}$ to the optical devices, the shortening of the $Ni^{III}-Ni^{III}$ distances is effective, which can afford increase of $\chi^{(3)}$ values. For this purpose, the simple ligands compared with chxn are more preferable. According to such a strategy, we have synthesized quasi-one-dimensional bromo-bridged Ni^{III} complexes with diaminopropane ligands, $[Ni(R\text{-}pn)_2Br]Br_2$ (*R*-pn = (*R*)-1,2-diaminopropane) and $[Ni(rac\text{-}pn)_2Br]Br_2$ (*rac*-pn = *rac*-1,2-diaminopropane). In the preceding paper, we have shown the direct observation of the disorders of the methyl groups in $[Ni(R\text{-}pn)_2Br]Br_2$ by STM.[15] As a result, the methyl groups are not disordered on the right-hand and left-hand sides alternatively, but make domain structures or fluctuated structures. In this paper, we will discuss the electronic states and structural disorders of $[Ni(R\text{-}pn)_2Br]Br_2$ and [Ni(*rac*-

(9) (a) Baeriswyl, D.; Bishop, A. R. *J. Phys. C* **1988**, *21*, 339−356. (b) Mishima, A.; Nasu, K. *Phys. Rev. B* **1989**, *40*, 5593−5597.
(10) Robin, M. B.; Day, P. *Adv. Inorg. Chem. Radiochem.* **1967**, *9*, 247−422.
(11) Toriumi, K.; Wada, Y.; Mitani, T.; Bandow, S.; Yamashita, M.; Fujii, Y. *J. Am. Chem. Soc.* **1989**, *111*, 2341−2342. (b) Toriumi, K.; Okamoto, H.; Mitani, T.; Bandow, S.; Yamashita, M.; Wada, Y.; Fujii, Y.; Clark, R. J. H.; Michael, D. J.; Edward, A. J.; Watkin, D.; Kurmoo, M.; Day, P. *Mol. Cryst. Liq. Cryst.* **1990**, *181*, 333−342.
(12) Okamoto, H.; Shimada, Y.; Oka, Y.; Chainani, A.; Takahashi, T.; Kitagawa, H.; Mitani, T.; Toriumi, K.; Inoue, K.; Manabe, T.; Yamashita, M. *Phys. Rev. B* **1996**, *54*, 8438−8445.
(13) (a) Okamoto, H.; Mitani, T.; Toriumi, K.; Yamashita, M. *Mater. Sci. Eng. B* **1992**, *13*, L9−L14. (b) Okamoto, H.; Mitani, T. *Prog. Theor. Phys.* **1993**, *113*, 191−201.
(14) Nasu, K. *J. Phys. Soc. Jpn.* **1984**, *52*, 3865−3873. (b) Iwano, K.; Nasu, K. *J. Phys. Soc. Jpn.* **1992**, *61*, 1380−1389. (c) Webber-Milbrodt, S. M.; Gammel, J. T.; Bishop, A. R.; Lor, E. Y., Jr. *Phys. Rev. B* **1992**, *45*, 6435−6458.
(15) Sasaki, M.; Takaishi, S.; Miyasaka, H.; Sugiura, K.; Yamashita, M. *J. Am. Chem. Soc.* **2005**, *43*, 14958−14959.

pn)$_2$Br]Br$_2$ by optical spectra, X-ray structural analyses, and STM measurements.

Experimental Section

Single crystals of [Ni(*R*-pn)$_2$Br]Br$_2$ and [Ni(*rac*-pn)$_2$Br]Br$_2$ were obtained by electrysis of [Ni(L)$_2$Br$_2$] (L = *R*-pn or *rac*-pn).[16] X-ray single-crystal structural analyses were made using Bruker SMART1000 diffractometer at 100 K. Polarized reflectivity spectra were obtained by using a specially designed spectrometer equipped with a 25-cm grating monochromator and an optical microscope. The electric field vector is chosen to be parallel to the 1D chain direction ($E||b$). The obtained reflectivity spectra were converted to the optical conductivity spectra by a Kramers−Kronig transformation. STM measurements were performed at room temperature and ambient pressure with mechanically sharpened Pt/Ir tips. Single crystals of the present compounds were cleaved and mounted onto a sample stage with carbon pastes so that the surface of the *bc* plane can be observed. STM images were acquired with the constant height mode using a JEOL JSPM-5200 microscope. A sample bias voltage (V_s) was chosen to be +1.1 V.

Results and Discussion

Figure 2 shows the single-crystal X-ray structure of [Ni(*rac*-pn)$_2$Br]Br$_2$ at 100 K.[17] Two *rac*-pn ligands are coordinating to the Ni^{III} ions to form the planer [Ni(*rac*-pn)$_2$] units. The [Ni^{III}(*rac*-pn)$_2$] units and bromide ions are arranged alternatively along the *b* axis, forming the linear chain structures. The unit cell parameters of [Ni(*rac*-pn)$_2$Br]Br$_2$ and [Ni(*R*-pn)$_2$Br]Br$_2$ are completely the same within error. The Ni−Ni distances of these compounds along the 1D chain are ca. 5.10 Å, which is the shortest among Ni−Br 1D chain compounds so far reported. The marked difference of crystal structure in the present two compounds is in the feature of structural disorder. In [Ni(*rac*-pn)$_2$Br]Br$_2$, the methyl groups, as well as the carbon atoms of the ethylene moieties of the *rac*-pn ligands, are disordered with half occupancies. The twisting motion of the ethylene moiety is prohibited because the methyl group is fixed in the equatorial direction. Therefore, the disorder of the ethylene moieties is not dynamic but statically (statistically) one, namely a 1:1 mixture of the *R*-pn and *S*-pn ligands are in the crystal, resulting in an achiral space group (*Immm*). On the other hand, there is no disorder in the ethylene moieties in [Ni(*R*-pn)$_2$Br]Br$_2$, affording a chiral spacegroup (*I*222), while the methyl groups of the *R*-pn ligands are still disordered. Such situations are illustrated in Figure 3.

Figure 4 shows the optical conductivity spectrum of [Ni(*R*-pn)$_2$Br]Br$_2$ together with that of [Ni(chxn)$_2$Br]Br$_2$.[12] The optical conductivity spectrum of [Ni(*R*-pn)$_2$Br]Br$_2$ showed an intense peak at ca. 1.3 eV, which is attributable to a CT transition from the bridging bromide ion to the upper

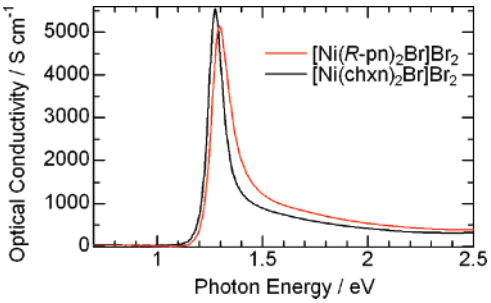

Figure 4. Optical conductivity spectra of [Ni(*R*-pn)$_2$Br]Br$_2$ and [Ni(chxn)$_2$Br]Br$_2$.

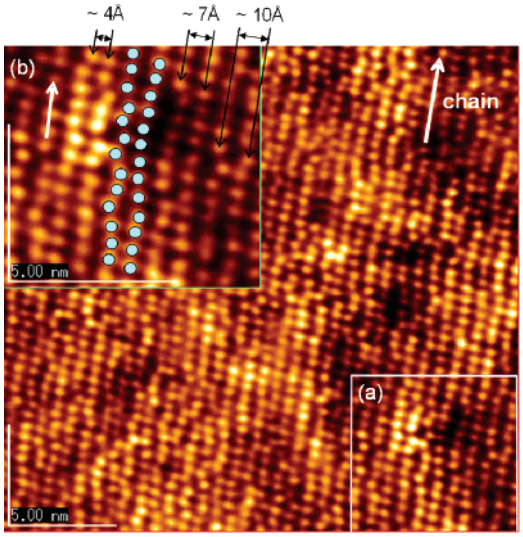

Figure 5. STM image of [Ni(*rac*-pn)$_2$Br]Br$_2$ on the *bc* plane (240 × 240 Å^2). The white arrow shows the 1D chain direction. (b)STM image of magnification of the square part of (a). The blue circles show bright spots arranged in a zigzag fashion.

Hubbard band of Ni. Such a situation is quite analogous to that of [Ni(chxn)$_2$Br]Br$_2$. Okamoto et al. have revealed that the *U* value is mainly characteristic of the metal ion itself and almost independent of the surroundings.[12] Therefore, the fundamental band structure is supposed to be the same as that of [Ni(chxn)$_2$Br]Br$_2$, as shown in Figure 1.

In order to observe the feature of the disorder in methyl group, we performed the STM measurements of [Ni(*rac*-pn)$_2$Br]Br$_2$. Figure 5 shows an STM image of [Ni(*rac*-pn)$_2$Br]Br$_2$ on the *bc* plane in the range of 240 × 240 Å^2. Bright spots are observed every 5 Å along the *b* axis (1D chain). Since the STM measurements were performed with the positive sample bias (V_s = +1.1 V), the tunnel current is observed from the Fermi energy (E_F) of a tip to a conduction band of the sample. According to the above discussion, the conduction band of the present complex is an unoccupied upper-Hubbard (UH) band composed of the d_{z^2} orbital of the Ni^{III} ions. Therefore, the tunnel current from the E_F of a tip to the UH band of the Ni^{III} is observed as bright spots. However, the bright spots are not completely linear, but are arranged in a zigzag fashion. The image of this compound is similar to that of [Ni(*R*-pn)$_2$Br]Br$_2$ but different from that of [Ni(chxn)$_2$Br]Br$_2$. In the previous paper, we clarified that the tunnel currents strongly reflect the electronic state of the

(16) A solution of [Ni(L)$_2$]Br$_2$ (L = *R*-pn or *rac*-pn) (60 mM) and saturated tetamethylammonium bromide in anhydrous 1-propanol was electrolyzed under the constant current of 10 μA for 2 weeks. Black prismatic single crystals were obtained at the anode. Anal. Calcd for $C_6H_{20}Br_3N_4Ni_1$: C, 16.13; H, 4.51; N, 12.54. Found: C, 16.00; H, 4.63; N, 12.58.

(17) Crystal data of [Ni(*rac*-pn)$_2$Br]Br$_2$: $C_6H_{20}Br_3N_4Ni_1$, M_r = 446.70, orthorhombic, *Immm*, T = 100 ± 2 K, a = 19.360(5) Å, b = 5.0951(12) Å, c = 6.9308(17) Å, V = 683.7(3) Å^3, Z = 2, ρ_{calcd} = 2.170, final R = 0.0359, R_w = 1.004, GOF = 1.191 with $I > 2.00\sigma(I)$.

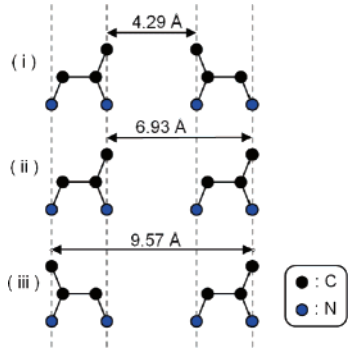

Figure 6. Interchain disordered patterns of the methyl groups.

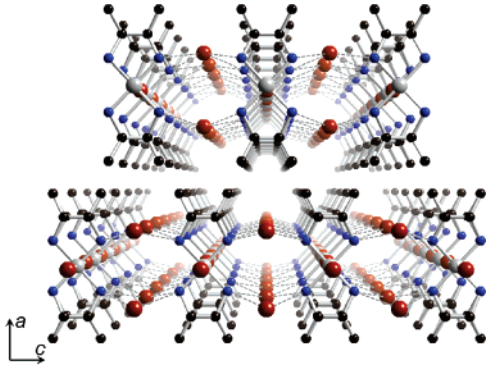

Figure 7. Perspective view of the crystal structure of [Ni(*rac*-pn)$_2$Br]Br$_2$ onto the *ac* plane. Hydrogen atoms are omitted for clarity. Dashed lines show hydrogen bonds between amino protons and bromide ions.

metal ions in the Ni−Pd mixed-metal compounds.[18] The bright spots, which are the methyl groups, are not arranged on the right- and left-hand side alternatively, but in the domain structures or fluctuated structure as observed in [Ni(*R*-pn)$_2$Br]Br$_2$ previously reported.[15]

Figure 6 shows the schematic geometry of the disordered methyl group. From the crystal structural data, distances between carbon atoms of the disordered methyl group of the neighboring chains along the *c* axis are evaluated to be 4.29, 6.93, and 9.57 Å when the disordered methyl group is located in the head-to-head(i), head-to tail(ii), and tail-to-tail(iii) fashions, respectively. By measuring the distance between neighboring bright spots along the *c* axis, we have succeeded in determining the local geometry of methyl groups of *rac*-pn ligands. Therefore, the tunnel currents should be observed through the methyl groups of pn ligands.

At this point, we can compare the configurations of the pn ligands in [Ni(*R*-pn)$_2$Br]Br$_2$ and [Ni(*rac*-pn)$_2$Br]Br$_2$. As shown in the X-ray crystal structures of these compounds, the methyl groups of pn ligands are disordered in both compounds. The STM images of both compounds are very similar to each other, because the oxidation states of both compounds are the same (Ni^{III} states) and the tunnel currents are observed through the methyl groups. The marked structural difference between the two present compounds is in the disorder of the ethylene moieties in the pn ligands, that is, the disorder in [Ni(*rac*-pn)$_2$Br]Br$_2$ and no disorder in [Ni(*R*-pn)$_2$Br]Br$_2$. However, since the circumstances of the methyl groups in both pn compounds are similar to each other, the tunnel currents are the same and the STM images of these compounds are observed similarly.

Finally, we discuss the difference between the electronic structure of bulk crystal and crystalline surface. Strictly speaking, the electronic structure of the crystalline surface is different from that of bulk crystal because the chemical and physical environments are different from each other. Atomic rearrangements sometimes occur so as to reduce the surface energy, e.g., 7 × 7 structure of silicon crystal. In the present system, there are relatively strong chemical bonds within the *bc* plane, i.e., −Br−Ni−Br− strong covalent bond along the *b* axis[19] and NH···Br···HN-type hydrogen bond within the *bc* plane, whereas along *a* axes, there are only weak van der Waals contacts, as shown in Figure 7. Therefore, the environment of the crystalline surface is considered not to be so different from that of the bulk crystal. Actually, we have measured STM images of Ni−Pd mixed-metal compounds [Ni$_{1-x}$Pd$_x$(chxn)$_2$Br]Br$_2$ and succeeded in explaining the images by the electronic structure of the bulk crystals.[18]

Acknowledgment. This work was partly supported by a Grant-in Aid for Creative Scientific Research from the Ministry of Education, Culture, Sports, Science and Technology.

Supporting Information Available: Crystal structure of [Ni(*rac*-pn)$_2$Br]Br$_2$ (CIF). This material is available free of charge via the Internet at http://pubs.acs.org.

IC700379M

(18) Takaishi, S.; Miyasaka, H.; Sugiura, K.; Yamashita, M.; Matsuzaki, H.; Kiahida, H.; Okamoto, H.; Tanaka, H.; Marumoto, K.; Ito, H.; Kuroda, S.; Takami, T. *Angew. Chem., Int. Ed.* **2004**, *43*, 3171−3175.

(19) Takaishi, S.; Tobu, Y.; Kitagawa, H.; Goto, A.; Shimizu, T.; Okubo, T.; Mitani, T.; Ikeda, R. *J. Am. Chem. Soc.* **2004**, *126*, 1614−1615.